Lignin Upgrading Hot Paper

How to cite: *Angew. Chem. Int. Ed.* **2021**, *60*, 8976–8982
International Edition: doi.org/10.1002/anie.202015431
German Edition: doi.org/10.1002/ange.202015431

Selectively Upgrading Lignin Derivatives to Carboxylates through Electrochemical Oxidative C(OH)–C Bond Cleavage by a Mn-Doped Cobalt Oxyhydroxide Catalyst

*Hua Zhou[+], Zhenhua Li[+], Si-Min Xu, Lilin Lu, Ming Xu, Kaiyue Ji, Ruixiang Ge, Yifan Yan, Lina Ma, Xianggui Kong, Lirong Zheng, and Haohong Duan**

Abstract: *Oxidative cleavage of C(OH)–C bonds to afford carboxylates is of significant importance for the petrochemical industry and biomass valorization. Here we report an efficient electrochemical strategy for the selective upgrading of lignin derivatives to carboxylates by a manganese-doped cobalt oxyhydroxide (MnCoOOH) catalyst. A wide range of lignin-derived substrates with C(OH)-C or C(O)-C units undergo efficient cleavage to corresponding carboxylates in excellent yields (80–99%) and operational stability (200 h). Detailed investigations reveal a tandem oxidation mechanism that base from the electrolyte converts secondary alcohols and their derived ketones to reactive nucleophiles, which are oxidized by electrophilic oxygen species on MnCoOOH from water. As proof of concept, this approach was applied to upgrade lignin derivatives with C(OH)-C or C(O)-C motifs, achieving convergent transformation of lignin-derived mixtures to benzoate and KA oil to adipate with 91.5% and 64.2% yields, respectively.*

Introduction

Carboxylic acids represent an important class of compounds in the fine and bulk chemical industry with wideapplications as food preservatives, pharmaceuticals, and building blocks of polymers.[1] Most of these commodities are currently produced from fossil-derived hydrocarbons via tandem oxidation (Scheme 1a). Alternatively, lignin, a main constituent of biomass, offers a sustainable source to alleviate the petroleum depleting and associated environmental issues.[2] Notably, carbohydrates and lignin features C(OH)-C motifs,[3] therefore providing a feasible route to carboxylic acids via selective C–C bonds cleavage (Scheme 1b). In this respect, several thermocatalytic methods have been recently developed for aerobic oxidative cleavage of C(OH)–C bonds, achieving efficient transformation of lignin models to corresponding carboxylic acids.[2b–d] Nevertheless, these processes often require homogeneous catalysts (e.g., copper or vanadium) or toxic nitrogen oxides, and are operated at elevated temperature (Table S1).[2c,d,4] Therefore, the development of more sustainable procedures for oxidative transformation of C(OH)–C bonds in lignin and its derivatives to produce carboxylic acids continues to attract significant interest.

Electrochemical oxidation provides a promising alternative to synthesize value-added organic oxygenates instead of oxygen evolution reaction (OER). Advantageously, the thermodynamically favorable anodic organic oxidation facil-

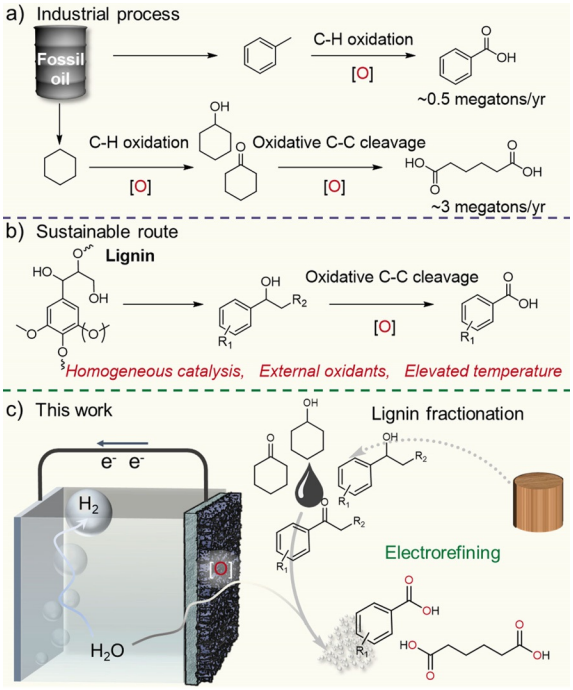

Scheme 1. a) Industrial processes for the production of carboxylic acids. b) Oxidative C(OH)-C cleavage of lignin derivatives. c) Proposed electrochemical strategy for upgrading lignin-derived platform molecules coupled with HER.

[*] Dr. H. Zhou,[+] K. Ji, Dr. R. Ge, Prof. H. Duan
Department of Chemistry, Tsinghua University
Beijing 100084 (China)
E-mail: hhduan@mail.tsinghua.edu.cn
Prof. Z. Li,[+] Dr. S.-M. Xu, Prof. M. Xu, Y. Yan, Dr. L. Ma, Dr. X. Kong
State Key Laboratory of Chemical Resource Engineering
College of Chemistry, Beijing University of Chemical Technology
Beijing 100029 (China)
Dr. L. Lu
School of Chemistry and Chemical Engineering
Wuhan University of Science and Technology
Wuhan 430081 (China)
Dr. L. Zheng
Institute of High Energy Physics, Chinese Academy of Sciences
Beijing 100049 (China)
[+] These authors contributed equally to this work.
Supporting information and the ORCID identification number(s) for the author(s) of this article can be found under: https://doi.org/10.1002/anie.202015431.

itates the improvement of energy efficiency of the overall electrolysis paired with cathodic half reactions, for example, hydrogen evolution reaction (HER) and CO_2 reduction.[5] To that end, much research interests have focused on exploring oxidative transformation of organic molecules.[5b,6] Among them, biomass platform chemicals have received special concern for carboxylic acids production from primary alcohols.[5b,7] Despite these efforts, the electrochemical oxidation of lignin-derived products via oxidative C(OH)−C bonds cleavage is underexplored possibly due to its high binding dissociation energy (260–300 kJ mol^{-1}).[8]

Herein we report an electrochemical oxidation strategy for selective upgrading of lignin-derived secondary alcohols or ketones into carboxylates over a MnCoOOH catalyst integrated with water splitting (Scheme 1 c). The MnCoOOH catalyst shows good generality to various secondary alcohols and ketones to corresponding carboxylates in satisfactory yield (64–99 %) and excellent operational stability (200 h) at room temperature without external oxidant. Comprehensive studies indicate that the process involves tandem nucleophilic oxidation reactions (NOR). The base from alkaline electrolyte drives the deprotonation of alcohols and ketones to reactive nucleophiles (i.e., alkoxide and carbanion, respectively), which are subsequently oxidized by electrophilic oxygen species over MnCoOOH prior to OER. As proof of concept, this strategy is efficient for electrorefining diverse lignin aromatics and KA oil featuring C(OH)-C and C(O)-C units to benzoate and adipate in high yields, respectively (91.5 % and 64.2 %).

Results and Discussion

Cobalt-oxyhydroxide (CoOOH) is a promising anodic material for electrochemical oxidation,[9] and recognized to be the catalytically active phase of Co-based catalysts during anodic reactions such as OER[10] and organic transformations.[11] In addition, high-valence metallic heteroatoms doping, such as Mn[12] and Fe,[10c] has shown to be an efficient strategy to modulate the electronic structure of CoOOH and thereby to enhance the intrinsic activity. Considering these facts, we prepared Mn-doped CoOOH supported on nickel foam (MnCoOOH/NF) as anode to investigate electrochemical oxidative cleavage of C(OH)−C bonds. As illustrated in Figure 1 a, the MnCoOOH/NF was synthesized firstly using an electrodeposition method to obtain Mn-doped $Co(OH)_2$ on NF ($MnCo(OH)_2$/NF), followed by cyclic voltammetry (CV) activation. Specifically, the generated local OH^- ions on the surface of NF electrode under negative potential (−1 V vs. SCE) mainly reacted with Co cations in aqueous metal solution (200 mM Co^{2+} and 100 M Mn^{2+}) and led to $MnCo(OH)_2$/NF. The low content (atomic Mn/Co ratio ≈ 1/20) of Mn in $MnCo(OH)_2$/NF is attributed to that Mn^{2+} ions prone to be oxidized and deposited on the counter electrode (Table S2). Then, the as-obtained $MnCo(OH)_2$/NF material was activated in 1 M KOH electrolyte using CV method (1.0–1.8 V vs. RHE, 20 cycles) to give the desired MnCoOOH/NF. The comparative CoOOH/NF sample was also synthesized using the similar method except the absence of Mn.

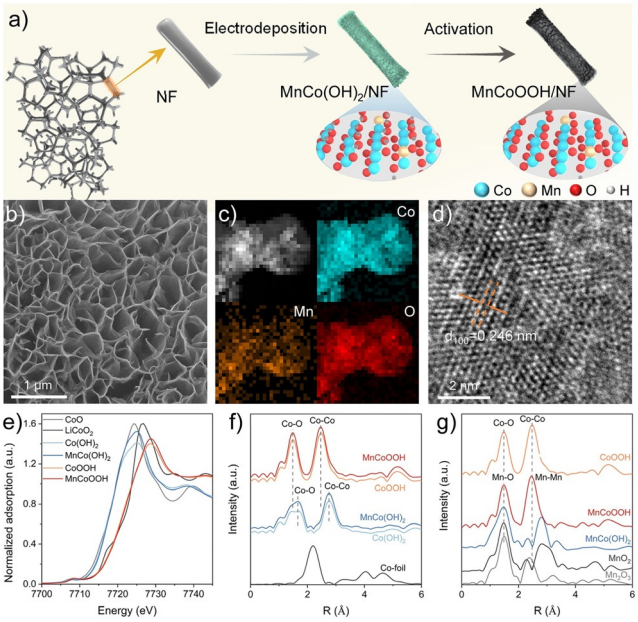

Figure 1. a) Schematic illustration of the synthesis of MnCoOOH/NF. b) SEM image, c) EDS mapping, and d) HR-TEM of MnCoOOH. e) Normalized XANES adsorption profiles and f) EXAFS Fourier transform (FT) spectra of Co *K*-edge for samples. g) EXAFS spectra of Co *K*-edge for CoOOH and Mn *K*-edge for Mn-based samples.

X-ray diffraction (XRD) patterns indicate that γ-phase MnCoOOH/NF and CoOOH/NF were successfully prepared by CV activation of α-phase $MnCo(OH)_2$/NF and $Co(OH)_2$/NF, respectively through anodic deprotonation process (Figure S1).[9c,10c] Scanning electron microscope (SEM) analysis shows the honeycomb-like array structure composed of MnCoOOH nanosheets (Figure 1 b), which display thinner average thickness (9.3 nm) than that of CoOOH (31.2 nm), suggesting Mn doping have effect on limiting the growth of $Co(OH)_2$ at *c* orientation (Figures S2,3). Energy dispersive spectrometry (EDS) mapping shows that Mn is uniformly distributed on MnCoOOH nanosheets (Figure 1 c). High-resolution transmission electron microscope (HR-TEM) image of MnCoOOH (Figure 1 d) displays an interplanar spacing of 0.246 nm, which corresponds to the (110) plane of hexagonal γ-CoOOH.[9c] We further investigated the electronic structure of $MnCo(OH)_2$, MnCoOOH, and the counterparts using X-ray absorption near-edge structure (XANES), extended X-ray absorption fine structure spectroscopy (EXAFS), and X-ray photoelectron spectroscopy (XPS). As shown in Figure 1 e, the Co K-edge adsorption edges of both $MnCo(OH)_2$ and $Co(OH)_2$ are coincident with that of CoO reference, reflecting the prominence of Co^{2+} species in the two materials. Upon the CV activation applied, the adsorption edges of MnCoOOH and CoOOH shift positively and are next to that of $LiCoO_3$, indicating the formation of Co^{3+} species as corroborated by Co2p XPS results (Figure S4a). The oxidation of metal cations in basal plane contributes to deprotonation of the hydroxyls of the α-phase to form O-bridged metal-oxygen-metal (M-O-M) moieties (Figure S4b) and contraction of the local Co-O and Co-Co distances.[9b,10c] EXAFS analysis confirm this trend

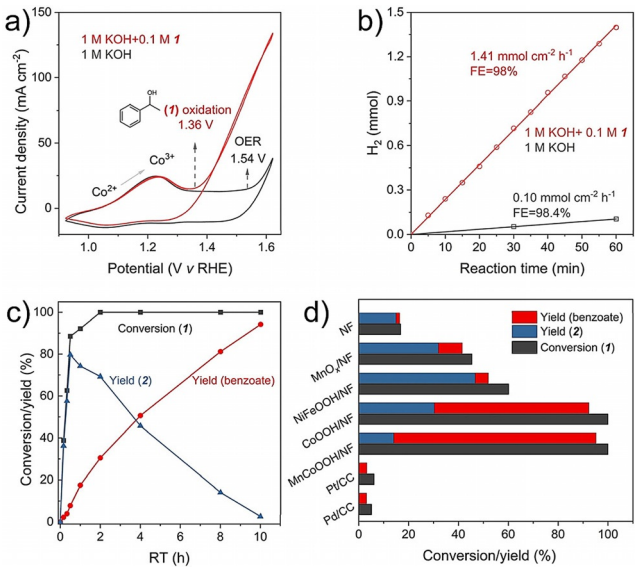

Figure 2. Electrochemical evaluation. a) Cyclic voltammetric (CV) curves of MnCoOOH/NF in 1 M KOH with or without **1** at a scan rate of 10 mV s^{-1}. b) Cathodic H_2 evolution at 1.5 V vs. RHE in 1 M KOH with or without **1**. c) Kinetic curves for **1** transformation as a function of reaction time. Reaction conditions: 0.5 mmol **1**, 50 mL 1 M KOH, MnCoOOH/NF(+)//Pt foil(−), 1.5 V vs. RHE. d) Comparison of the catalytic performances of other common catalysts and MnCoOOH/NF. Reaction conditions: 0.5 mmol **1**, 50 mL 1 M KOH, anodic catalyst-(+)//Pt foil(−), 1.5 V vs. RHE, 8 h.

toward shorter distance of first shell Co-O and second shell Co-Co (Figure 1 f). Moreover, the Mn K-edge EXFAS spectra show that the length of Mn-O and Mn-Mn in MnCoOOH are equal to that of Co-O and Co-Co, respectively (Figure 1 g). Therefore, it can be deduced that Mn atoms replaced Co atoms to form octahedral structure in the MnCoOOH.[12] Overall, these characterization techniques comprehensively identify the successful synthesis of metal oxyhydroxide structure of MnCoOOH and CoOOH.

The as-prepared samples were initially evaluated for electrochemical oxidation of 1-phenylethanol (denoted as **1**), a typical lignin model compound with C(OH)-C structure,[2b–d] in undivided cell with 1 M KOH electrolyte. As shown in Figure 2 a, the CV curve of MnCoOOH/NF shows the good OER activity in 1.0 M KOH electrolyte with an onset overpotential of 310 mV. To our delight, introducing **1** into the electrolyte lead to significant reduction of onset potential to 130 mV, indicating the lower energy barrier of **1** oxidation than that of OER. As a result, the cathodic H_2 production rate increased from 0.1 mmol cm^{-2} h^{-1} of traditional water splitting to 1.41 mmol cm^{-2} h^{-1} at 1.5 V vs. RHE (Figure 2 b), leading to the enhancement of the energy efficiency of the whole process.[5c] Notably, the MnCoOOH catalyst exhibits approximately twofold improvement in current density for **1** oxidation, compared with CoOOH under constant potential (1.5 V vs. RHE) (Figure S5). This can be partially explained by the increased electrochemical active surface area of MnCoOOH (3.3 mF cm^{-2}) compared to that of CoOOH (1.6 mF cm^{-2}) (Figure S6). Moreover, electrochemical impedance spectroscopy reveal that Mn doping induces significant decrease of charge transfer resistance for MnCoOOH catalyst (Figure S7).

To have an insight into the reaction process, the distribution of **1** and its derivatives upon the course of reaction time were analyzed by high-performance liquid chromatography (HPLC). As shown in Figure S8, the HPLC chromatograms demonstrate that acetophenone (**2**) is the only observable intermediate of **1** before the formation of final product-benzoate. Kinetic curves show that **1** undergoes rapid oxidation (88.5 %) in 30 minutes at 1.5 V vs. RHE, giving 79.7 % of **2** and 7.8 % of benzoate (Figure 2 c) with a total faradaic efficiency of 85.3 % (Figure S9). Subsequently, **2** is gradually converted into benzoate and formate, achieving maximum benzoate yield (94.2 %) after 10 hours reaction (Figure 2 c and Figure S9). These results reveal the reaction pathways of anodic **1** oxidation over MnCoOOH/NF involves two key steps: i. dehydrogenation of secondary alcohol (**1**) to ketone (**2**), and ii. ketone mediated oxidative C−C bond cleavage to carboxylates. Notably, no benzoate is detected when using ethylbenzene as substrate under the same reaction conditions (Figure S10), highlighting the key role of C(OH)-C and C(O)-C for scissoring C−C bonds in this process. To the best of our knowledge, the transformation of **1** to benzoate using an electrochemical strategy has not been reported previously, thus offer a sustainable alternative to conventional thermo-driven processes performed at elevated temperature using external oxidants (Table S1).

To confirm the unique activity of MnCoOOH/NF, we prepared and evaluated the catalytic performances of other common catalysts (Figures S11–15 and Figure 2 d), including non-precious metal oxy(hydroxides) on NF (MnO_x/NF, NiFeOOH/NF) and noble-metal nanocrystals on carbon cloth (Pt/CC and Pd/CC). As shown in Figure 2 d, NF and MnO_x/NF give much lower conversion of **1** (16.8 % and 45.4 %, respectively) than that of CoOOH/NF (> 99 %) and MnCoOOH/NF (> 99 %), indicating the high intrinsic activity of Co-based oxyhydroxide. As for the well-known OER catalyst in alkaline media, NiFeOOH/NF, the conversion of **1** and the selectivity of benzoate are much inferior to that of the MnCoOOH/NF, suggesting the different reaction mechanism of **1** oxidation and OER processes. Moreover, both Pt/CC and Pd/CC catalysts give poor conversion (< 7 %), and benzoate is the only detected product. The low activity of Pt/CC and Pd/CC can be explained by the inefficient binding between the relatively hydrophobic metal surface and the substrate that contains numerous alkoxide groups in alkaline media.[13] The electrode material dependent activity for **1** oxidation reflects the nature of an inner-sphere reaction of this reaction, which require strong interaction between substrate and electrode for electron transfer.[14]

To have an insight into the mechanism of this reaction on MnCoOOH/NF electrode, we carried out isotope labeling experiments to investigate inappreciable intermediates during electrochemical **1** oxidation using alkaline H_2O, D_2O, and $H_2{}^{18}O$ electrolyte (1 M KOH), respectively. The isotopomer distribution in the intermediate (**2**) and benzoate were analyzed by mass spectrometry (MS) equipped on gas chromatography (GC). First, we notice that the H atom on OH group of **1** can spontaneously exchange with water under

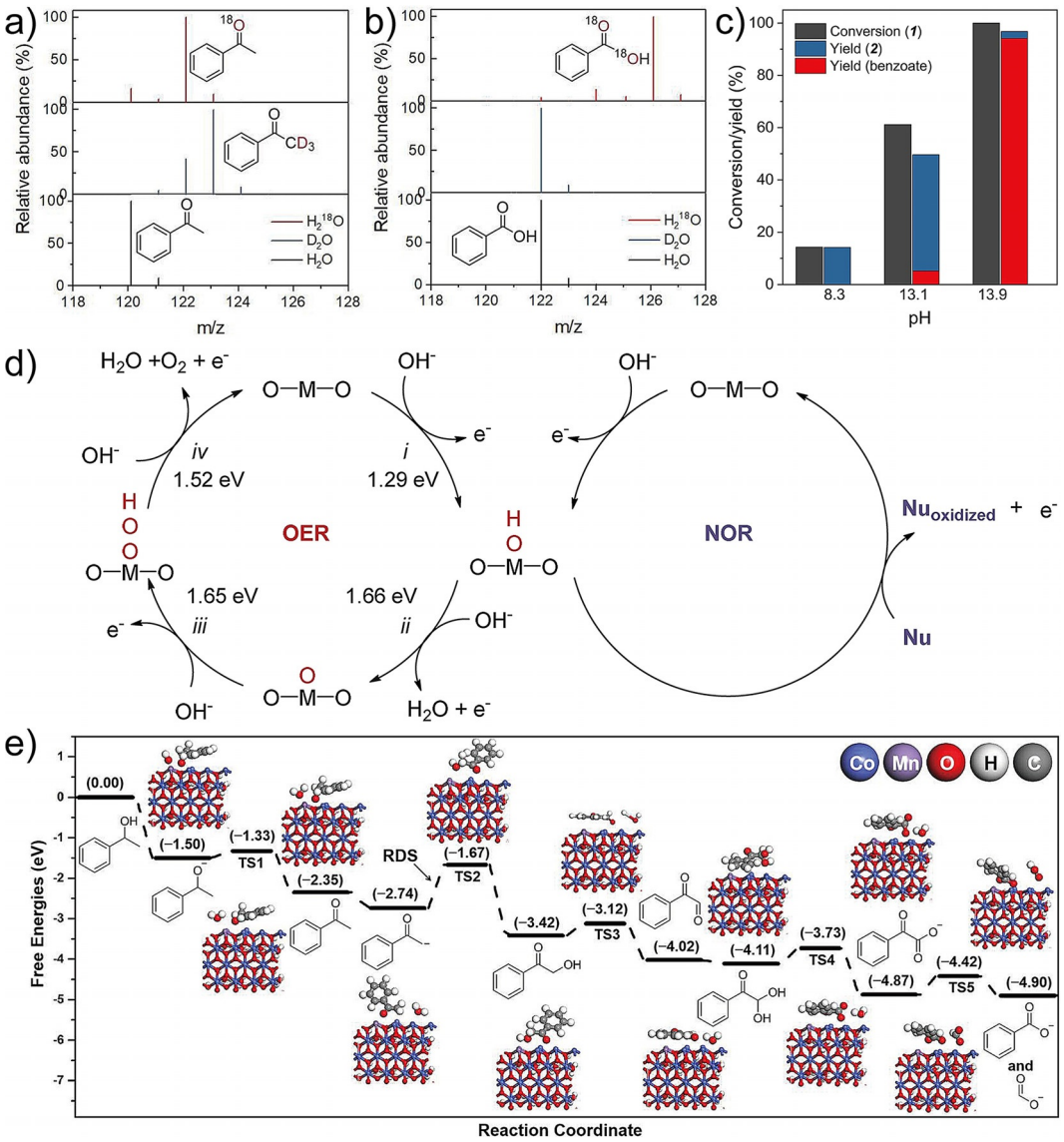

Figure 3. Mechanism study. a,b) Mass spectra of a) acetophenone ($m/z=120$) and b) benzoic acid ($m/z=122$) derived from **1** in isotope-labeled electrolyte. c) The effect of electrolyte pH on electrocatalytic oxidation of **1**. Reaction conditions: 0.5 mmol **1**, 50 mL 1 M KOH, MnCoOOH/NF(+)//Pt foil(−), 1.5 V vs. RHE, 10 h. d) Illustration of the formation of electrophiles for OER (red oxygen species represent electrophiles)[16] and NOR. e) Free energy diagram for electrocatalytic oxidation of **1** over MnCoOOH catalyst.

reaction conditions, suggesting the formation of alkoxide via acid-base equilibrium (Figure S16 a–c). Moreover, the MS spectra of **2** show that one ^{18}O atom from $H_2{}^{18}O$ and three D atoms from D_2O are incorporated into as-formed **2** from **1** oxidation (Figure 3a and Figure S16 a). The plausible reasons for the results are base promoted reversible ketone hydration and keto-enol tautomerism, respectively (Figure S16d, e, detailed analysis shown in SI). Notably, these results reveal the formation of nucleophilic intermediates (alkoxide and carbanion) from **1** and **2** by deprotonation in the presence of base (Figure S16d, e, and S17). Simultaneously, the MS spectra of benzoic acid reveal that two ^{18}O atoms in benzoate are originated from ^{18}O labeled water (Figure 3b), suggesting that water derived oxygen species involved in this reaction.

We recognize that these results are different from a recent publication of Lei and co-workers,[6e] who reported a neutral electrocatalytic process for selective **1** oxidation to **2** without C–C bond cleavage. Thus, we investigated the influence of pH on the reaction rates and product distribution of electrochemical **1** oxidation over MnCoOOH/NF and CoOOH/NF under our reaction conditions (Figure 3c and Figure S18). The results show that in near neutral electrolyte (pH 8.3), **1** is quantitatively converted into **2** with moderate reaction rate without C–C bond cleavage, which is in agreement with Lei's results. However, both the conversion of **1** and the selectivity to benzoate are dramatically increased with higher pH (pH 13.9). These results suggest that high concentration of hydroxide ions promotes both the dehydrogenation of **1** and subsequent C(O)-C cleavage process. The pH-dependent

reactivity could be explained by the high pK_a of **1** (14.4) and **2** (18.4), which requires high pH to drive their deprotonation to nucleophilic alkoxide and carbanion, respectively.[15]

Nucleophilic oxidation reaction (NOR) mechanism is wildly adopted in inner-sphere OER or organic reaction over anode, where molecules react with interfacial oxidizing species.[14,17] Significantly, electrophilic oxygen species (i.e. OH*, O*, OOH*) have been identified on the anodic catalysts surface during alkaline OER process by experiments and/or theoretical calculations.[9c,12,16,18] It is well demonstrated that the rate-determining-step over Co-based hydroxides or oxyhydroxides is the deprotonation of adsorbed OH* to O* (step *ii*),[19] being consistent with our density functional theory (DFT) calculations over MnCoOOH catalyst (Figure 3d, left circle and Figures S19,20). In our work, the applied working potential can only overcome the energy barrier of generating OH* (1.29 eV), rather than that of deprotonation of OH* (1.66 eV). Therefore, we infer that OH* is the main electrophile on the surface of MnCoOOH/NF during **1** transformation because of the relatively low working potential (1.5 V vs. RHE). While, compound **1** and its derived intermediates nucleophilic attack on OH* over MnCoOOH/NF (Figure 3d, right cycle), along with proton-electron transfers. To validate this assumption, we performed DFT calculations for **1** oxidation towards benzoate. As shown in Figure 3e, **1** can smoothly transforms to a carbanion, which further reacts with OH* on MnCoOOH/NF to give 2-hydroxyacetophenone (**3**). In addition, compound **3** is gradually transformed into final benzoate, via 2-oxo-2-phenylacetaldehyde (**4**) and benzoylformic acid (**5**) intermediates, which are verified by experiments (Figure S21). Notably, the calculated RDS of the tandem nucleophilic oxidation processes is the conversion of **2**-derived carbanion to **3** (1.07 eV), which is in agreement with experimentally kinetic curves (Figure 2c).

On the basis of the above results and previous literatures, we propose a tandem NOR pathways for electrochemical transformation of **1** to benzoate in alkaline electrolyte. As shown in Figure 4, the secondary alcohol initially undergoes H_α deprotonation into more active alkoxide via base catalysis, which is then oxidized by the electrophilic OH* on the surface of MnCoOOH for β-H elimination to corresponding ketone (**2**).[15a,16] Then the hydroxide ions induce keto-enol tautomerization of **2** to enol via carbanion intermediate. The nucleophilic attack of carbanion intermediate to electrophilic OH* on MnCoOOH generates α-ketol (**3**). Subsequently, **3** is converted to **4** via electrocatalytic dehydrogenation. Then, the base from electrolyte promotes the reversible transformation of **4** to reactive geminal diol for electrocatalytic dehydrogenation to **5**, which is followed by an oxidative C–C cleavage process to generate benzoate and formate as the final products.[6c,20]

Recent publications have shown that doping of high-valence Mn^{4+} with an unpaired $3d^3$ configuration into Co is an effective method that is capable of extracting local electrons from Co sites, then reducing the adsorption free energy of CoOOH for OH^-, therefore leading to enhanced OER performance.[12] In our work, Mn K-edge XANES reveal that the valence of Mn dopants mainly exist in +3 in $MnCo(OH)_2$ and +4 in MnCoOOH (Figure S22a). Consistent with the previous study, high-valence Mn-doping results in the increase of white line peak intensity of MnCoOOH compared to CoOOH (Figure S22b), suggesting a relatively stronger adsorption of the OH^- ions for the formation of electrophilic OH* species, which accounts for the enhanced activity of MnCoOOH, together with the above-mentioned higher electrochemical active surface area (Figure S5) and lower charge transfer resistance (Figure S6).

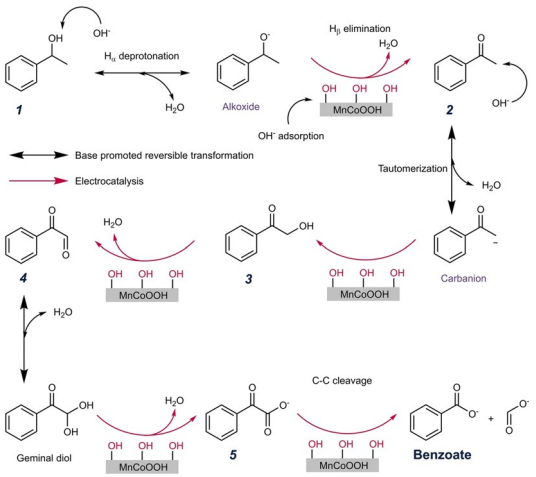

Figure 4. A plausible tandem nucleophilic oxidation reaction (NOR) mechanism for electrochemical oxidation of **1**.

To demonstrate the generality of this electrochemical process, a wide range of lignin model compounds with C(OH)-C or C(O)-C motifs were examined as substrates using MnCoOOH/NF catalyst under the established reaction conditions. As shown in Figure 5, excellent yields (84.1–99.2%) of benzoate are obtained from benzylic compounds (**2**, **3**–**7**, **13**, **14**). In addition, the electrochemical oxidation of substrates with substituent groups on phenyl, such as methyl (**11**), methoxy (**8**–**10**, **15**), carbonyl (**12**), also afford satisfactory yield (80.1–96.7%) to substituted benzoates. Moreover, this approach also exhibits excellent catalytic results for oxidizing primary alcohols (**16** and **18**) and aldehydes (**17** and **18**) to corresponding carboxylic acids with near theoretical

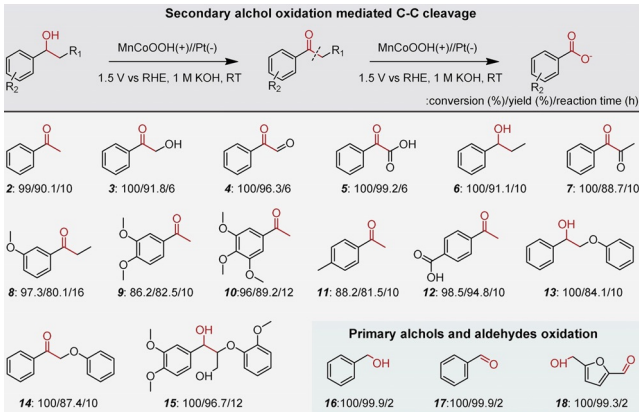

Figure 5. Substrate scope investigation.

yield. For example, 99.3 % yield of 2,5-furandicarboxylic acid, an emerging renewable substitute of terephthalic acid,[21] can be obtained from biomass-derived 5-hydroxymethylfurfural (**18**) via this electrocatalytic strategy in 2 h.

Moreover, we evaluated the long-term stability of MnCoOOH/NF electrode for anodic oxidation of **1** in batch reactions. As shown in Figure S23, the conversion of **1** and yield of benzoate remain stable after 20 batches (200 h), which is possibly attributed to the self-supporting structure of MnCoOOH/NF. In addition, the SEM images and XPS spectra of the fresh and used MnCoOOH/NF anode demonstrate the morphological and chemical structure stability under reaction conditions (Figures S24,25).

A significant issue for lignin valorization is downstream processing of lignin-derived products to commercial commodities, with the advancements in lignin fractionation.[22] For example, selective oxidation has been demonstrated to be an effective route for lignin fractionation (Figure 6a), leading to heterogenous portfolio of molecules include aromatic ketones, aldehydes, and acids featuring C_α(O)-R (R = H, OH, C(O)Me, CH_3, C_2H_5).[3] However, the purification of these chemicals with similar property remains a huge challenge. In this context, we demonstrated the convergent transformation of a mixture composed of 11 kinds of aromatic substrates (**1**–**7**, **13**, **14**, **16**, **17**, as shown in Figure 5) with benzylic C_α(OH)-R or C_α(O)-R motifs using our electrochemical strategy. As shown in Figure 6b, these lignin models with different functional groups are convergently transformed into benzoate with 91.5 % yield. Notably, benzoate is an important commodity chemical that is conventionally produced by oxidation of petroleum-based toluene at elevated temperature and pressure (150–170 °C, 1 MPa).[7a] Therefore, our electrochemical strategy provides an efficient approach to convergently transform these diverse lignin-derived products into relatively single commodity, acting an "electrochemical funnel".

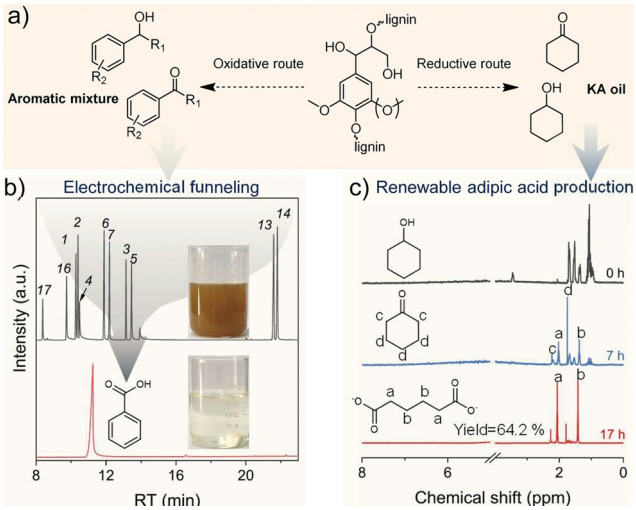

Figure 6. a) Schematic illustration of lignin fractionation to platform molecules. b) Total ion chromatograms of various lignin model compounds (top) and derived benzoic acid (bottom) after electro-funneling. Inset pictures are the electrolyte before and after electro-funneling. Reaction conditions: 0.1 mmol of each substrate, 50 mL 1 M KOH, MnCoOOH/NF(+)//Pt foil(−), 1.5 V vs. RHE, 12 h. c) ^{1}H NMR spectra of cyclohexanol and its derived products during electrolysis. Reaction conditions: 1 mmol cyclohexanol, 50 mL 1 M KOH, MnCoOOH/NF(+)//Pt foil(−), 1.45 V vs. RHE, 17 h.

On the other hand, KA oil is an important platform chemical that can be produced from lignin-derived phenols or aromatic ethers via reductive routes (Figure 6a).[23] Considering the C(OH)-C and C(O)−C bonds exist in KA oil, we expect our electrochemical strategy could also exhibit catalytic activity in their oxidative transformation. The catalytic results show that the starting cyclohexanol was tandemly converted to adipate via cyclohexanone intermediate, as demonstrated by ^{1}H NMR spectra (Figure 6c). NMR and HPLC analysis show that 100 % conversion of cyclohexanol and 64.2 % yield of adipate is achieved. This work provides a sustainable way to produce adipate, a monomer of nylon 66 which has wide applications. Although the selectivity to adipate in this preliminary study requires further optimization, this electrochemical strategy offers a promising route to produce monomer of polymers from renewable biomass.

Conclusion

In summary, we synthesized a Mn-doped CoOOH electrocatalyst, which can selectively upgrade lignin derivatives into carboxylates through electrochemical oxidative C(OH)−C bonds cleavage. Detailed mechanistic studies indicate that base catalyzed the deprotonation of secondary alcohols and its derived ketones to reactive nucleophiles, which subsequently oxidized by electrophilic OH adsorbed on the surface of MnCoOOH. This methodology can be generalized to various lignin derivatives with C(OH)-C or C(O)-C motifs for producing carboxylic acids in high yield. As proof of concept, this process demonstrated its applications in electro-funneling lignin-derived mixture products into single benzoate and transforming lignin-derived KA oil to adipate with high efficiency. We believe this work provides a promising avenue toward carboxylates via C(OH)-C and C(O)−C bonds cleavage under mild and environmentally-benign conditions.

Acknowledgements

This work was supported by the National Natural Science Foundation of China (Grant No. 21978147, 21935001, 22090031). The authors thank the BL1W1B in the Beijing Synchrotron Radiation Facility (BSRF).

Conflict of interest

The authors declare no conflict of interest.

Keywords: carboxylic acids · C−C bond cleavage · electrochemical oxidation · hydrogen evolution · lignin upgrading

[1] a) R. Sang, P. Kucmierczyk, R. Duhren, R. Razzaq, K. Dong, J. Liu, R. Franke, R. Jackstell, M. Beller, *Angew. Chem. Int. Ed.* **2019**, *58*, 14365 – 14373; *Angew. Chem.* **2019**, *131*, 14503 – 14511; b) Z. Zhang, G. W. Huber, *Chem. Soc. Rev.* **2018**, *47*, 1351 – 1390.

[2] a) S. Song, J. Zhang, G. Gozaydin, N. Yan, *Angew. Chem. Int. Ed.* **2019**, *58*, 4934 – 4937; *Angew. Chem.* **2019**, *131*, 4988 – 4991; b) H. Luo, L. Wang, S. Shang, G. Li, Y. Lv, S. Gao, W. Dai, *Angew. Chem. Int. Ed.* **2020**, *59*, 19268 – 19274; *Angew. Chem.* **2020**, *132*, 19430 – 19436; c) M. Liu, Z. Zhang, J. Song, S. Liu, H. Liu, B. Han, *Angew. Chem. Int. Ed.* **2019**, *58*, 17393 – 17398; *Angew. Chem.* **2019**, *131*, 17554 – 17559; d) M. Liu, Z. Zhang, J. Yan, S. Liu, H. Liu, Z. Liu, W. Wang, Z. He, B. Han, *Chem* **2020**, *6*, 3288 – 3296; e) Z. Cai, J. Long, Y. Li, L. Ye, B. Yin, L. J. France, J. Dong, L. Zheng, H. He, S. Liu, S. C. E. Tsang, X. Li, *Chem* **2019**, *5*, 2365 – 2377.

[3] a) X. Wu, X. Fan, S. Xie, J. Lin, J. Cheng, Q. Zhang, L. Chen, Y. Wang, *Nat. Catal.* **2018**, *1*, 772 – 780; b) A. Rahimi, A. Ulbrich, J. J. Coon, S. S. Stahl, *Nature* **2014**, *515*, 249 – 252; c) W. Lan, J. Behaghel de Bueren, J. Luterbacher, *Angew. Chem. Int. Ed.* **2019**, *58*, 2649 – 2654; *Angew. Chem.* **2019**, *131*, 2675 – 2680.

[4] a) L. Zhang, X. Bi, X. Guan, X. Li, Q. Liu, B. D. Barry, P. Liao, *Angew. Chem. Int. Ed.* **2013**, *52*, 11303 – 11307; *Angew. Chem.* **2013**, *125*, 11513 – 11517; b) H. Liu, C. Dong, Z. Zhang, P. Wu, X. Jiang, *Angew. Chem. Int. Ed.* **2012**, *51*, 12570 – 12574; *Angew. Chem.* **2012**, *124*, 12738 – 12742; c) M. Wang, J. Lu, L. Li, H. Li, H. Liu, F. Wang, *J. Catal.* **2017**, *348*, 160 – 167; d) H. Liu, M. Wang, H. Li, N. Luo, S. Xu, F. Wang, *J. Catal.* **2017**, *346*, 170 – 179; e) S. K. Hanson, R. T. Baker, J. C. Gordon, B. L. Scott, D. L. Thorn, *Inorg. Chem.* **2010**, *49*, 5611 – 5618; f) H.-R. Tian, Y.-W. Liu, Z. Zhang, S.-M. Liu, T.-Y. Dang, X.-H. Li, X.-W. Sun, Y. Lu, S.-X. Liu, *Green Chem.* **2020**, *22*, 248 – 255.

[5] a) P. De Luna, C. Hahn, D. Higgins, S. A. Jaffer, T. F. Jaramillo, E. H. Sargent, *Science* **2019**, *364*, eaav3506; b) Y. X. Chen, A. Lavacchi, H. A. Miller, M. Bevilacqua, J. Filippi, M. Innocenti, A. Marchionni, W. Oberhauser, L. Wang, F. Vizza, *Nat. Commun.* **2014**, *5*, 4036; c) S. Verma, S. Lu, P. J. A. Kenis, *Nat. Energy* **2019**, *4*, 466 – 474; d) X. Wei, Y. Li, L. Chen, J. Shi, *Angew. Chem. Int. Ed.* **2021**, *60*, 3148 – 3155; *Angew. Chem.* **2021**, *133*, 3185 – 3192.

[6] a) M. Bajada, S. Roy, J. Warnan, K. Abdiaziz, A. Wagner, M. Roessler, E. Reisner, *Angew. Chem. Int. Ed.* **2020**, *59*, 15633 – 15641; *Angew. Chem.* **2020**, *132*, 15763 – 15771; b) Y. Li, X. Wei, L. Chen, J. Shi, *Angew. Chem. Int. Ed.* **2021**, https://doi.org/10.1002/anie.202009854; *Angew. Chem.* **2021**, https://doi.org/10.1002/ange.202009854; c) Y. Li, X. Wei, L. Chen, J. Shi, M. He, *Nat. Commun.* **2019**, *10*, 5335; d) W. J. Liu, Z. Xu, D. Zhao, X. Q. Pan, H. C. Li, X. Hu, Z. Y. Fan, W. K. Wang, G. H. Zhao, S. Jin, G. W. Huber, H. Q. Yu, *Nat. Commun.* **2020**, *11*, 265; e) D. Wang, P. Wang, S. Wang, Y. H. Chen, H. Zhang, A. Lei, *Nat. Commun.* **2019**, *10*, 2796; f) Y. Lum, J. E. Huang, Z. Wang, M. Luo, D.-H. Nam, W. R. Leow, B. Chen, J. Wicks, Y. C. Li, Y. Wang, C.-T. Dinh, J. Li, T.-T. Zhuang, F. Li, T.-K. Sham, D. Sinton, E. H. Sargent, *Nat. Catal.* **2020**, *3*, 14 – 22.

[7] a) H. Huang, C. Yu, X. Han, H. Huang, Q. Wei, W. Guo, Z. Wang, J. Qiu, *Energy Environ. Sci.* **2020**, *13*, 4990 – 4999; b) B. You, X. Liu, N. Jiang, Y. Sun, *J. Am. Chem. Soc.* **2016**, *138*, 13639 – 13646; c) H. G. Cha, K. S. Choi, *Nat. Chem.* **2015**, *7*, 328 – 333; d) S. Wang, N. Zhang, L. I. Tao, W. E. I. Chen, L. Zhou, Z. Liu, B. O. Zhou, G. E. N. Huang, Y. Zou, H. Lin, *Angew. Chem. Int. Ed.* **2019**, *58*, 15895 – 15903; *Angew. Chem.* **2019**, *131*, 16042 – 16050; e) P. Zhang, X. Sheng, X. Chen, Z. Fang, J. Jiang, M. Wang, F. Li, L. Fan, Y. Ren, B. Zhang, B. J. J. Timmer, M. S. G. Ahlquist, L. Sun, *Angew. Chem. Int. Ed.* **2019**, *58*, 9155 – 9159; *Angew. Chem.* **2019**, *131*, 9253 – 9257; f) M. Rafiee, M. Alherech, S. D. Karlen, S. S. Stahl, *J. Am. Chem. Soc.* **2019**, *141*, 15266 – 15276; g) L. Zhang, R. Chen, J. Luo, J. Miao, J. Gao, B. Liu, *Nano Res.* **2016**, *9*, 3388 – 3393.

[8] M. Wang, F. Wang, *Adv. Mater.* **2019**, *31*, 1901866.

[9] a) R. Subbaraman, D. Tripkovic, K. C. Chang, D. Strmcnik, A. P. Paulikas, P. Hirunsit, M. Chan, J. Greeley, V. Stamenkovic, N. M. Markovic, *Nat. Mater.* **2012**, *11*, 550 – 557; b) A. Bergmann, T. E. Jones, E. Martinez Moreno, D. Teschner, P. Chernev, M. Gliech, T. Reier, H. Dau, P. Strasser, *Nat. Catal.* **2018**, *1*, 711 – 719; c) J. Huang, J. Chen, T. Yao, J. He, S. Jiang, Z. Sun, Q. Liu, W. Cheng, F. Hu, Y. Jiang, Z. Pan, S. Wei, *Angew. Chem. Int. Ed.* **2015**, *54*, 8722 – 8727; *Angew. Chem.* **2015**, *127*, 8846 – 8851.

[10] a) E. Fabbri, M. Nachtegaal, T. Binninger, X. Cheng, B. J. Kim, J. Durst, F. Bozza, T. Graule, R. Schaublin, L. Wiles, M. Pertoso, N. Danilovic, K. E. Ayers, T. J. Schmidt, *Nat. Mater.* **2017**, *16*, 925 – 931; b) S. Song, J. Zhou, X. Su, Y. Wang, J. Li, L. Zhang, G. Xiao, C. Guan, R. Liu, S. Chen, H.-J. Lin, S. Zhang, J.-Q. Wang, *Energy Environ. Sci.* **2018**, *11*, 2945 – 2953; c) F. Dionigi, Z. Zeng, I. Sinev, T. Merzdorf, S. Deshpande, M. B. Lopez, S. Kunze, I. Zegkinoglou, H. Sarodnik, D. Fan, A. Bergmann, J. Drnec, J. F. Araujo, M. Gliech, D. Teschner, J. Zhu, W. X. Li, J. Greeley, B. R. Cuenya, P. Strasser, *Nat. Commun.* **2020**, *11*, 2522.

[11] L. Ma, H. Zhou, M. Xu, P. Hao, X. Kong, H. Duan, *Chem. Sci.* **2020**, https://doi.org/10.1039/D1030SC05499B.

[12] Y. Huang, X. Zhao, F. Tang, X. Zheng, W. Cheng, W. Che, F. Hu, Y. Jiang, Q. Liu, S. Wei, *J. Mater. Chem. A* **2018**, *6*, 3202 – 3210.

[13] D. W. Wakerley, M. F. Kuehnel, K. L. Orchard, K. H. Ly, T. E. Rosser, E. Reisner, *Nat. Energy* **2017**, *2*, 17021.

[14] A. J. Bard, *J. Am. Chem. Soc.* **2010**, *132*, 7559 – 7567.

[15] a) Y. Kwon, S. C. Lai, P. Rodriguez, M. T. Koper, *J. Am. Chem. Soc.* **2011**, *133*, 6914 – 6917; b) Y. Chiang, A. J. Kresge, J. Wirz, *J. Am. Chem. Soc.* **1984**, *106*, 6392 – 6395.

[16] H. B. Tao, Y. Xu, X. Huang, J. Chen, L. Pei, J. Zhang, J. G. Chen, B. Liu, *Joule* **2019**, *3*, 1498 – 1509.

[17] a) H. N. Nong, L. J. Falling, A. Bergmann, M. Klingenhof, H. P. Tran, C. Spori, R. Mom, J. Timoshenko, G. Zichittella, A. Knop-Gericke, S. Piccinin, J. Perez-Ramirez, B. R. Cuenya, R. Schlogl, P. Strasser, D. Teschner, T. E. Jones, *Nature* **2020**, *587*, 408 – 413; b) W. Chen, C. Xie, Y. Wang, Y. Zou, C.-L. Dong, Y.-C. Huang, Z. Xiao, Z. Wei, S. Du, C. Chen, B. Zhou, J. Ma, S. Wang, *Chem* **2020**, *6*, 2974 – 2993.

[18] N. Zhang, X. Feng, D. Rao, X. Deng, L. Cai, B. Qiu, R. Long, Y. Xiong, Y. Lu, Y. Chai, *Nat. Commun.* **2020**, *11*, 4066.

[19] I. C. Man, H. Y. Su, F. Calle-Vallejo, H. A. Hansen, J. I. Martínez, N. G. Inoglu, J. Kitchin, T. F. Jaramillo, J. K. Nørskov, J. Rossmeisl, *ChemCatChem* **2011**, *3*, 1159 – 1165.

[20] X. Han, H. Sheng, C. Yu, T. W. Walker, G. W. Huber, J. Qiu, S. Jin, *ACS Catal.* **2020**, *10*, 6741 – 6752.

[21] H. Zhou, H. Xu, Y. Liu, *Appl. Catal. B* **2019**, *244*, 965 – 973.

[22] S. S. Wong, R. Shu, J. Zhang, H. Liu, N. Yan, *Chem. Soc. Rev.* **2020**, *49*, 5510 – 5560.

[23] a) Y. Liao, S.-F. Koelewijn, G. Van den Bossche, J. Van Aelst, S. Van den Bosch, T. Renders, K. Navare, T. Nicolaï, K. Van Aelst, M. Maesen, H. Matsushima, J. Thevelein, K. Van Acker, B. Lagrain, D. Verboekend, B. F. Sels, *Science* **2020**, *367*, 1385 – 1390; b) H. Liu, T. Jiang, B. Han, S. Liang, Y. Zhou, *Science* **2009**, *326*, 1250 – 1252; c) H. Duan, N. Yan, R. Yu, C. R. Chang, G. Zhou, H. S. Hu, H. Rong, Z. Niu, J. Mao, H. Asakura, T. Tanaka, P. J. Dyson, J. Li, Y. Li, *Nat. Commun.* **2014**, *5*, 3093; d) Q. Meng, M. Hou, H. Liu, J. Song, B. Han, *Nat. Commun.* **2017**, *8*, 14190; e) Y. L. Zhou, Y. J. Gao, X. Zhong, W. B. Jiang, Y. L. Liang, P. F. Niu, M. C. Li, G. L. Zhuang, X. N. Li, J. G. Wang, *Adv. Funct. Mater.* **2019**, *29*, 1807651.

Manuscript received: November 18, 2020
Revised manuscript received: January 18, 2021
Accepted manuscript online: February 8, 2021
Version of record online: March 10, 2021

